1994

The Role of Thallium as a Hydrogen Entry Promoter on Cathodically Polarized HY-130 Steel

G. Zheng
University of South Carolina - Columbia

Branko N. Popov
University of South Carolina - Columbia, popov@engr.sc.edu

Ralph E. White
University of South Carolina - Columbia, white@cec.sc.edu

Publication Info

Journal of the Electrochemical Society, 1994, pages 1526-1532.

Publisher's link: http://dx.doi.org/10.1149/1.2054957
DOI: 10.1149/1.2054957

24. J. L. Roberts, Jr., T. S. Calderwood, and D. T. Sawyer, *ibid.*, **105,** 7691 (1983).
25. H. Sugimoto, S. Matsumoto, and D. T. Sawyer, *Environ. Sci. Technol.*, **22,** 1182 (1988).
26. T. Nagaoka, T. Sakai, K. Ogura, and T. Yoshino, *Anal. Chem.*, **58,** 1953 (1986).
27. T. Nagaoka, T. Fukunaga, T. Yoshino, I. Watanabe, T. Nakayama, and S. Okazaki, *ibid.*, **60,** 2766 (1988).
28. J. Schreurs, J. Van den Berg, A. Wonders, and E. Barendrecht, *Recl. Trav. Chim. Pays-Bas.*, **103,** 251 (1984).
29. G. E. Cabaniss, A. A. Diamantis, W. R. Murphy, Jr., R. W. Linton, and T. J. Meyer, *J. Am. Chem. Soc.*, **107,** 1845 (1985).
30. T. Nagaoka, T. Sakai, K. Ogura, and T. Yoshino, *J. Chem. Soc. Faraday Trans. 1,* **83,** 1823 (1987).
31. T. Fujinaga and S. Kihara, *CRC Critical Reviews in Analytical Chemistry,* **6,** 223 (1977).
32. T. Fujinaga, S. Okazaki, and T. Yamada, *Chem. Lett.*, 863 (1972).
33. D. R. Lowde and J. O. Williams, *J. Chem. Soc. Faraday Trans. 1,* **75,** 2312 (1979).
34. J. F. Rusling, *Acc. Chem. Res.*, **24,** 75 (1991).
35. E. Couture, J. F. Rusling, and S. Zhang, *ICHEME Symp. Ser.*, 177 (1992).
36. M. Hosono and H. Arai, *Kokai Tokkyo Koho,* 509 (1992).

The Role of Thallium as a Hydrogen Entry Promoter on Cathodically Polarized HY-130 Steel

G. Zheng,* B. N. Popov, and R. E. White****

Department of Chemical Engineering, University of South Carolina, Columbia, South Carolina 29208

ABSTRACT

Hydrogen permeation experiments were carried out to investigate the effect of thallium on hydrogen entry into HY-130 steel. These experiments show that the presence of thallium ions in an electrolyte drastically increase the hydrogen entry rate. The hydrogen entry efficiency and hydrogen surface coverage were increased by a factor of 10 and 6, respectively. In order to fit the permeation experimental data, the Iyer-Pickering-Zamanzadeh (I-P-Z) hydrogen permeation model was modified by including a mass-transfer term in the discharging equation. The relationship between hydrogen permeation and the hydrogen evolution reaction were investigated and new relationships were obtained.

Certain elements, particularly those of Group V-A (As, Sb, P) and VI-A (S, Te, Se) kinetically increase the rate of hydrogen entry into iron, steel, and ferritic alloys. Very small additions of these elements, referred to as "promoters" or "poisons" poison the hydrogen evolution reaction and consequently promote hydrogen absorption. Other species, which increase the hydrogen entry, are cyanide ions in alkaline solutions, halide ions in acidic solutions, and, under some circumstances (with much weaker effects), salts of heavy metals, such as Hg, Sn, and Pb. Extensive literature can be found on promoters. However, the results presented and the suggested reaction mechanism by different authors are conflicting. Shuler and Laidler[1] suggest that the promoter action could be due to an increasing of the strength of the M-H bond so that the activation energy for hydrogen recombination increased. Contrary to Shuler and Laidler's mechanism Bockris *et al.*,[2] Newman and Shreir,[3] and Kovba and Bagatskaya[4] suggest that the metal to hydrogen bond is reduced in the presence of the promoting species. The kinetic effect can be described by the decreased metal hydrogen bond energy which has a lower activation energy for the absorption process relative to the energy barrier for the recombination process. According to Smialowski, Szklarska-Smialowska *et al.*[5-8] the enhanced hydrogenation effect, in the presence of promoters, involves the formation of a stable hydride. By using various promoters in 1*N* H_2SO_4 and measuring the elongation of hydrogen-charged iron wires or coils, they found that the relative effectiveness of the promoter element correlated well with increasing bond strength and stability of the hydride (H_2S > PH_3 > AsH_3). Newman and Shreir[3] reached the same conclusion as Smialowski.[5] They galvanostatically charged high-strength steel specimens for 24 h and measured the hydrogen content afterwards. According to Newman and Shreir,[3] an enhanced hydrogen permeation occurs in the case of stable hydrides, such as AsH_3, PH_3, H_2S, and H_2Se. Smialowski's explanation was also supported by McGraw *et al.*[9] and Fontana and Staehle.[10] It is assumed that the hydrides first chemisorbed and then dissociated[11,12] on the metal surface and have the ability to transmit hydrogen atoms through the electrolyte/metal boundary. However, Radhakrishnan and Shreir[13] found that AsH_3, produced outside their permeation cell, did not enhance the hydrogen permeation rate when bubbled into the cell. The discrepancy in the necessity of the presence of arsine in these two papers[3,9] was confirmed by McCright and Stahle.[14] They found that the reduction of arsenate to elemental arsenic suppresses the hydrogen reaction and promotes the entry of hydrogen into steel structures during cathodic polarization. According to these authors the rate of entry of hydrogen does not depend on arsine (AsH_3) formation. The greatest relative permeation occurred in the potential range where arsenic is the stable phase. Some authors[15-17] suggested that the promoter interferes with the recombination step by increasing the average residence time of H on the surface which increases the surface coverage of adsorbed hydrogen. Alikin[18] and Beloglazov and Polukarov[19] have postulated that colloidal particles, which are formed during electrolysis promote hydrogen entry and that in the presence of poisons, hydrogen enters the metals as protons.

As shown in previous publications, the mechanism of promoter action is highly controversial. In this work, hydrogen permeation experiments were carried out to investigate the effect of thallium on hydrogen entry into HY-130 steel. We have established the atomic thallium rather than its hydride has a significant effect on hydrogen entry.

Experimental

Using the Devanathan-Stachurski permeation technique,[20,21] the rate of hydrogen permeation through HY-130 steel membrane was measured continuously as a function of time. The permeation experiments were carried out in a system with two compartments separated by a bipolar HY-130 steel membrane. The permeation rate through a thin membrane of thickness 0.15 mm was measured by setting

* Electrochemical Society Student Member.
** Electrochemical Society Active Member.

the potential on the "diffusion side" of the membrane (the side from which the hydrogen emerges) at a fixed value (−0.3 V *vs.* Hg/HgO). This value corresponds to almost a zero concentration of absorbed atomic hydrogen on the surface. This condition occurred when all hydrogen atoms which have diffused through the membrane and emerged on the diffusion side have been instantaneously ionized. The hydrogen permeation rate was directly proportional to the anodic current, which can be measured conveniently with a high degree of accuracy and sensitivity. The steel membrane on the cathodic side of the cell was polarized potentiostatically. Prior to the permeation studies the steel membrane was mechanically polished with 600 grade sand-paper and 0.5 μm high purity alumina powder to a mirror finish. The steel membrane was then cleaned in an ultrasonic cleaning bath and saturated with hydrogen in a 0.1*N* H_2SO_4 solution maintaining the solution at cathodic current density of 10 mA/cm^2 for 10 h. Then, the membrane was removed from the cell, etched for 20 s in a solution containing methyl alcohol and 1% H_2SO_4, rinsed with deionized water, dried in air, and fitted into the permeation cell.

To avoid possible passivation, the anodic side of the membrane was electroplated with a thin layer (0.15 to 0.20 μm) of palladium. The deposition was carried out in an electrolyte containing $2 \times 10^{-5}M$ $Na_2Pd(NO_2)_4$ using a current density of 100 μA/cm^2 for 2 h. Then, the electrolyte was drained off, and the compartment was washed with deionized water and filled with the anodic solution (0.2*M* NaOH). To keep the electrolyte impurities at the lowest possible level, the anodic solution, was pre-electrolyzed for at least 24 h in a separate electrolytic cell before putting it in the permeation cell. In the anodic compartment, the electrolyte was kept at −0.3 V *vs.* Hg/HgO reference electrode until the background current was reduced to below 3 μA/cm^2. Then, the cathodic compartment was filled with a supporting electrolyte containing 0.5*M* Na_2SO_4 and 0.5*M* H_2SO_4. Prepurified nitrogen was bubbled through both compartments in order to keep the system free of dissolved oxygen. All potentials were reported *vs.* SCE unless otherwise mentioned.

Results and Discussion

Hydrogen permeation studies on cathodically polarized HY-130 steel.—Permeation experiments were performed to clarify the relationship between thallium and hydrogen entry kinetics. Thallium was predeposited on a HY-130 steel membrane from electrolytes containing 0.5*M* Na_2SO_4 and 0.5*M* H_2SO_4 and $2 \times 10^{-2}M$ Tl^+. At cathodic potentials, more negative than −0.70 V, a visible deposition of thallium occurs on the steel surface. The open-circuit potential of the membrane with a predeposited thallium was −0.70 V. At applied potentials more positive than −0.70 V no bulk deposition of thallium was observed. Thus, in order to avoid bulk deposition of thallium on steel, most of the permeation experiments were performed at potentials more anodic than −0.70 V. The permeation experiment were also carried out on membranes with predeposited thallium on the surface and the results were compared with those obtained for underpotential deposited thallium.

The experiments were performed at different cathodic potentials in a solution containing 0.5*M* Na_2SO_4 and H_2SO_4 which is free of thallium ions. Initially, the membrane was charged at a potential of −0.5 V and then charged at more negative potentials using steps of 50 mV until the potential reached a value of −0.65 V. Thus, the applied potentials were: −0.50, −0.55, −0.60, and −0.65 V. After the permeation rate stabilized, at an applied potential of −0.65 V, the potential was switched off, and the decaying curve was created. The atomic hydrogen permeation current density *vs.* time at different potentials is plotted in Fig. 1. Figure 1 shows that the steady-state hydrogen permeation current increased with the increasing of the applied cathodic potential. The hydrogen diffusivity through HY-130 membrane was calculated by fitting the whole hydrogen permeation transient obtained experimentally for $E_{app} = -0.55$ V.

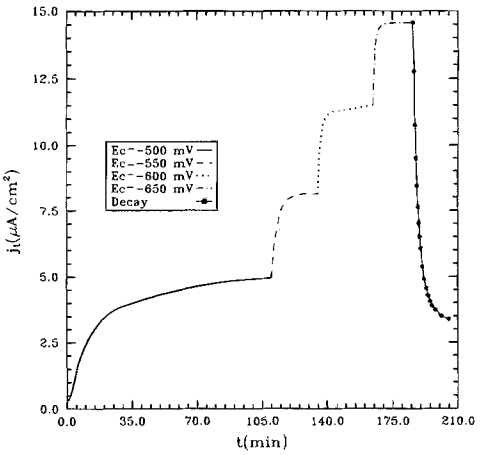

Fig. 1. Hydrogen permeation transients through a HY-130 steel membrane at different applied potentials in the absence of thallium ions in the electrolyte containing 0.5*M* Na_2SO_4, 0.5*M* H_2SO_4, the thickness of the membrane = 0.15 mm.

The experimental data fits the theoretical solution for hydrogen permeation through a membrane at a constant hydrogen concentration at the entry side of the membrane[22] with $D = 2.4 \times 10^{-7}$ cm^2/s.

Using the mechanistic model developed by Iyer, Pickering, and Zamanzadel, the I-P-Z model, the hydrogen surface coverage and the surface concentration, the hydrogen absorption, discharge, and recombination rate constants as well as the hydrogen evolution reaction (h.e.r.) coverage-dependent transfer coefficient, α_c and the exchange current density i_o may be computed from a knowledge of the steady-state hydrogen permeation current, cathodic charging current, hydrogen diffusivity, and hydrogen overvoltage. This was done by assuming that (*i*) the hydrogen evolution reaction is a coupled discharge-recombination process (*ii*) since $\eta >> RT/F$, hydrogen atom oxidation can be neglected; (*iii*) the Langmuir isotherm is used to describe the hydrogen coverage of the substrate; (*iv*) the intermediate hydrogen adsorption-absorption reaction is in local equilibrium; and (*v*) the hydrogen permeation process is described by a simple diffusion model through the membrane. With these assumptions, one can derive the following relationships[23]

$$i_c = i_0' (1 - \theta_s) e^{-a\alpha_c\eta} \quad [1]$$

$$i_r = F k_3 \theta_s^2 \quad [2]$$

$$j_\infty = \frac{FD}{L} c_s = \frac{c_s}{b} \quad [3]$$

$$j_\infty = F[k_{abs}\theta_s - k_{ads} c_s (1 - \theta_s)] \quad [4]$$

$$c_s = k'' \frac{\theta_s}{1 - \theta_s} \approx k'' \theta_s \quad [5]$$

$$k'' = \frac{k_{abs}}{k_{abs} + \frac{D}{L}} \quad [6]$$

$$\theta_s = \frac{b j_\infty}{k''} \quad [7]$$

$$j_\infty = \frac{k''}{b\sqrt{F k_3}} \sqrt{i_r} \quad [8]$$

$$i_c e^{a\alpha_c\eta} = -\frac{b i_0'}{k''} j_\infty + i_0' \quad [9]$$

where $i_r = i_c - j_\infty$ is the hydrogen recombination current density, i_c is the cathodic current density, j_∞ is the steady-state permeation flux, $b = L/FD$, L is the membrane thickness, F is the Faraday constant, D is the hydrogen diffusion coefficient, $a = F/RT$, α_c is the cathodic transfer coefficient, η is the overpotential, R is the gas constant, T is the temperature, C_s is the surface hydrogen concentration, θ_s is the

hydrogen surface coverage, k_3 is the recombination rate constant, k'' is the thickness dependent adsorption-absorption constant, $i_0' = i_0/1 - \theta_e$, where i_o is the exchange current density, k_{abs} is the absorption rate constant, and k_{ads} is the adsorption rate constant.

Due to the assumption that $i_c \approx i_r$, j_∞ is linearly related to $\sqrt{i_r}$.[24] This assumption is generally true because $j_\infty << i_c$ for most of the cases.

The Langmuir isotherm does not always apply, especially when hydrogen starts evolving. Frumkin-Temkin isotherm corrections have been used by Iyer *et al.*[25] in order to correct the hydrogen surface coverage for such reactions. In this case Eq. 1 and 2 become

$$i_c = i_0' (1 - \theta_s) e^{-a\alpha_c\eta} e^{-\alpha_c f \theta_s} \quad [10]$$

$$i_r = F k_3 \theta_s^2 e^{2\alpha_c f \theta_s} \quad [11]$$

respectively. The value 4.5 for $f = \gamma/RT$ is used when the surface is covered by hydrogen.[30] Substituting Eq. 7 into 10 and 11, the following modified I-P-Z relationships can be obtained

$$\ln\left(\frac{\sqrt{i_r}}{j_\infty}\right) = \frac{\alpha_c f b}{k''} j_\infty + \ln\left(\frac{b\sqrt{F k_3}}{k''}\right) \quad [12]$$

and

$$\ln\left(\frac{i_c e^{\frac{\alpha_c f b j_\infty}{k''}}}{1 - \frac{b j_\infty}{k''}}\right) = -\alpha_c a \eta + \ln i_0' \quad [13]$$

Equations 8 and 9, 12 and 13 may be used to evaluate various reactions parameters such as k_3, k'', and i_0' by plotting corresponding experimental data.

The steady-state hydrogen permeation current density (j_∞) and the cathodic current density (i_c) are plotted *vs.* hydrogen overpotential (η) in Fig. 2. The permeation current density (j_∞) *vs.* the square root of hydrogen recombination current density ($\sqrt{i_r}$) is given in Fig. 3, where $i_r = i_c - j_\infty$. In Fig. 3, a linear dependence exists between j_∞ and $\sqrt{i_r}$, which fits Eq. 8. This indicates that the experimental data may satisfy the I-P-Z model under Langmuir isotherm coverage. If true, log i_c *vs.* η and log j_∞ *vs.* η should be two linear relationships, with slopes of $-d\eta/d \log i_c = -1/2\ d\eta/d \log j_\infty = 120$ mV/decade,[23,24] assuming a transfer coefficient $\alpha_c = 0.5$. However, Fig. 2 does not show two straight lines, the slope of $-d\eta/d \log i_c$ varies from 137 mV/decade for the first two points to 313 mV/decade for the last two points (the corresponding values of $-d\eta/d \log j_\infty$ changes from 237 to 644 mV/decade). The first two points give a slope of 137 mV/decade and is close to the theoretical dependence $-d\eta/d \log i_c = 120$ mV/decade. The deviation of the linear relations may be due to an invalid coverage isotherm assumption, transfer coefficient (α_c) dependence on overpotential, or hydrogen coverage dependence on overpotential. At higher potentials, assuming that Temkin isotherm rather than a Langmuir isotherm applies, the slope $-d\eta/d \log i_c$ should change from 120 to 180 mV/decade. The change in slope from 137 to 313 mV/decade of the experimental data does not support this assumption. If the transfer coefficient (α_c) is a function of overpotential,[26,27] then $\partial\alpha_c/\partial\eta > 0$ may explain the nonlinear behavior observed in Fig. 2. However, that will give a negative value of i_0' by fitting Eq. 9 proving this assumption is incorrect. Taking into account that the coverage of hydrogen is a function of potential, the I-P-Z model[23] may be used to evaluate the transfer coefficient α_c. Using this procedure, different values of α_c were obtained at different potentials.

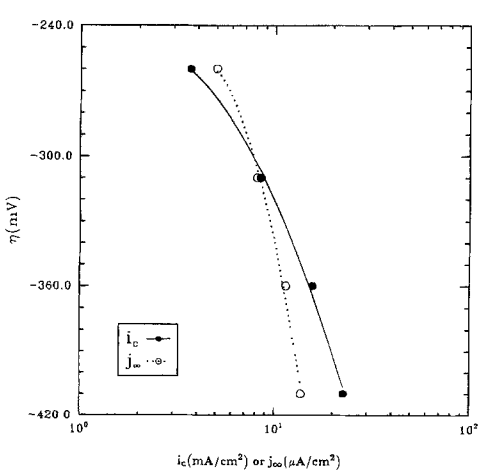

Fig. 2. The dependence of cathodic current density (i_c) and permeation current density (j_∞) upon cathodic overpotential (η) in the absence of thallium ions.

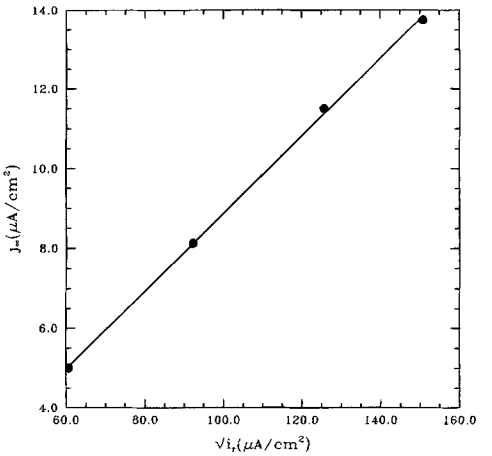

Fig. 3. Permeation current density (j_∞) *vs.* square root of recombination current density ($\sqrt{i_r}$) in the absence of thallium ions.

From Fig. 2 when the overpotential became more negative, the cathodic current approached a limiting value, which may be a mass transfer limiting current. Equation 1 uses the assumption that the mass-transfer rate is large enough or the current density is low enough so that the surface concentrations $C(x = 0)$ are close to the bulk concentrations (C^*). If the mass-transfer factor is taken into account, then Eq. 1 will become

$$i_c = i_0' (1 - \theta_s) \frac{C(x = 0)}{C^*} e^{-a\alpha_c\eta} \quad [14]$$

and according to Ref. 28

$$\frac{C(x = 0)}{C^*} = 1 - \frac{i_c}{i_l} \quad [15]$$

where i_l is the limiting current density. Inserting Eq. 15 into Eq. 14 and rearranging, one obtains

$$\frac{i_c i_l}{i_l - i_c} = i_0' (1 - \theta_s) e^{-a\alpha_c\eta} \quad [16]$$

and thus

$$\ln\left(\frac{i_c i_l}{i_l - i_c}\right) = \ln [i_0' (1 - \theta_s)] - a\alpha_c\eta \quad [17]$$

By fitting and extrapolating the experimental curve, $i_l = 29$ mA/cm^2. By plotting η *vs.* ln $[i_c i_l/(i_l - i_c)]$ in Fig. 4 and assuming that θ_s is close to zero and thereby negligible, the transfer coefficient α_c was computed to be 0.542 from the slope in Fig. 4.

If one includes mass-transfer effects, Eq. 9 becomes

$$\frac{i_c i_l}{i_o - i_c} e^{a\alpha\eta} = -\frac{b i_0'}{k''} j_\infty + i_0' \quad [18]$$

A plot of j_∞ *vs.* $[i_c i_l/(i_l - i_c)]\ e^{a\alpha_c\theta_s}$ is given in Fig. 5. From the intercept and slope, i_0' and k'' can be evaluated, respectively. These values are $i_0' = 18$ μA/cm^2 and $k'' = 6.6 \times 10^{-5}$ mol/cm^3. Assuming Eq. 8 is still applicable, the recombination constant k_3 can be obtained from the slope and was found to

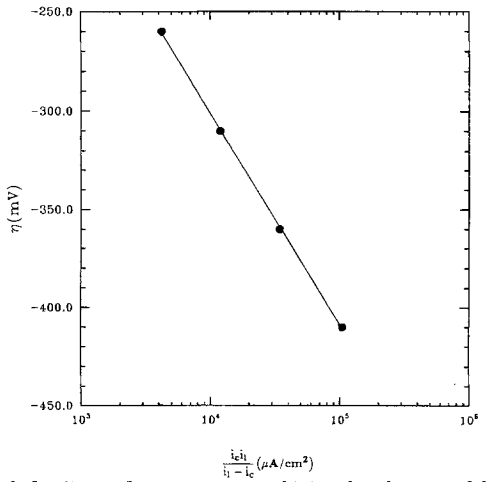

Fig. 4. ln $[i_c i_l/(i_l - i_c)]$ *vs.* overpotential (η) in the absence of thallium ions.

have a value of 1.1×10^{-5} mol/(cm² s). Using the Eq. 7, the hydrogen surface coverage changes from 0.05 to 0.14 when the overpotential changed from −0.26 to −0.43 V. This range of coverage is found by using the Langmuir isotherm assumption and assuming that it is reasonable to neglect θ_s in Eq. 1.

Hydrogen permeation on cathodically polarized HY-130 steel in the presence of thallium ions.—The permeation experiments, in the presence of thallium were repeated in the same electrolyte (0.5M Na_2SO_4, 0.5*M* H_2SO_4) in which 2×10^{-2}*M* of Tl^+ was added (in the form of Tl_2SO_4). In the presence of Tl^+ ions, the experiments were started at a potential of −0.50 V followed by an increase in potential in steps of −50 mV up to an applied potential of −0.65 V. The permeation transients are given in Fig. 6. In Fig. 6, the permeation current densities increase sharply compared with the results in Fig. 1 corresponding to the same applied potentials. Although the cathodic current density in the presence of thallium ions (not shown here) is decreased drastically, an abnormal permeation curve with a characteristic peak occurred when the applied potential reached −0.65 V. As discussed by Bockris and Subramanyan,[29] this anomalous behavior was caused by the spreading of microcracks after the hydrogen concentration reached a critical point. Higher cathodic applied potentials were used and the results are shown in Fig. 7. The permeation curve at a potential of −0.68 V is similar to the transient at −0.65 V. Both the maximum peak current and the steady-state current density are higher than the corresponding value at potential −0.650 V. When the potential was raised to −0.75 V, the permeation current density showed a sharp decrease compared with the current density obtained at −0.65 and at −0.68 V *vs.* SCE. The steady-state permeation current at −0.75 V is lower than the corresponding values at −0.65 and −0.68 V. This current density decrease was due to the bulk deposition of Tl^+ on the substrate. At −0.80 V, a similar (to −0.75 V) shape of transient was observed.

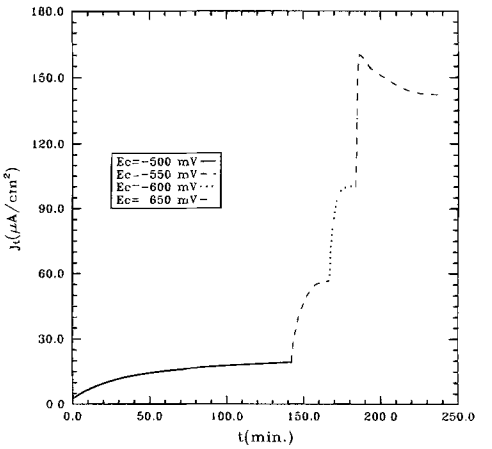

Fig. 6. Hydrogen permeation transients through HY-130 steel membrane at different applied potentials (−0.50 to −0.65 V *vs.* SCE) in the presence of 2×10^{-2}*M* of Tl^+ in the electrolyte containing 0.5*M* Na_2SO_4, 0.5*M* H_2SO_4, the thickness of the membrane = 0.15 mm.

In order to check whether the permeation current density increased due to possible surface preparation differences, the permeation experiments were repeated at potential −0.50 V in the absence of thallium ions in the electrolyte. After the permeation transient stabilized, the thallium ions in the form of Tl_2SO_4 were directly added to the solution to make 2×10^{-2}*M* of Tl^+. The permeation transients and cathodic current density are shown in Fig. 8 and 9, respectively. In the presence of Tl^+, the permeation current density increased by 74%. Apparently, the observed increase of the permeation current density is not due to the surface preparation. The permeation curves in Fig. 8 gave reproducible results compared with the corresponding results in Fig. 1 and 6. Figure 9 illustrates the significant suppression of the h.e.r. brought about by the addition of thallium. Initially, the sulfate electrolyte (0.5*M* Na_2SO_4 + 0.5*M* H_2SO_4) contained no thallium. At an applied constant potential of −0.50 V, the current density increased to a value of 3860 μA/cm². When thallium was added in the electrolyte, the cathodic current was reduced by 83%. The sharp reduction in h.e.r. was due to the kinetic limitations of the hydrogen discharge reaction on the deposited thallium monolayers.

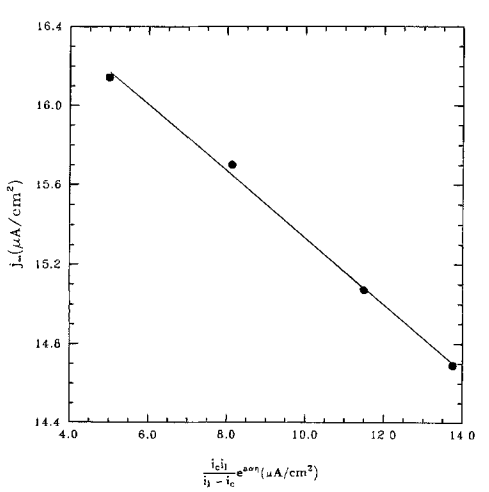

Fig. 5. ln $[i_c i_l/(i_l - i_c)]$ $e^{\alpha\alpha\eta}$ *vs.* permeation current density (j_∞) in the absence of thallium ions.

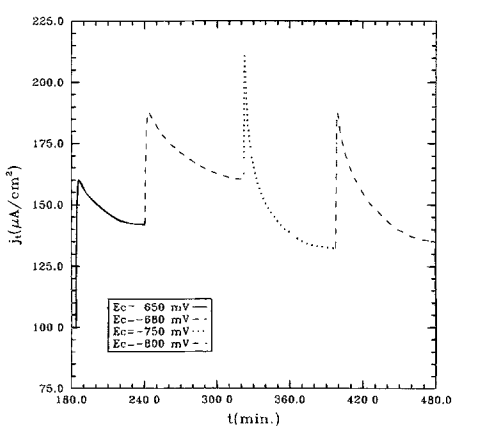

Fig. 7. Hydrogen permeation transients through HY-130 steel membrane at different applied potentials (−0.65 to −0.80 V *vs.* SCE) in the presence of 2×10^{-2}*M* of Tl^+ in the electrolyte containing 0.5*M* Na_2SO_4, 0.5*M* H_2SO_4, the thickness of the membrane = 0.15 mm.

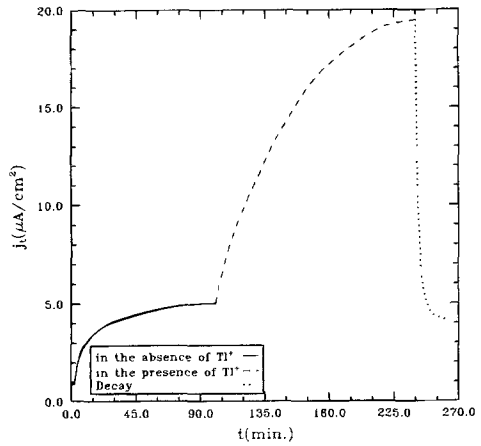

Fig. 8. Hydrogen permeation transients through HY-130 steel membrane at applied potentials of −0.50 V *vs.* SCE in the absence and presence of $2 \times 10^{-2}M$ of Tl^+ in the electrolyte containing 0.5*M* Na_2SO_4, 0.5*M* H_2SO_4, the thickness of the membrane = 0.15 mm.

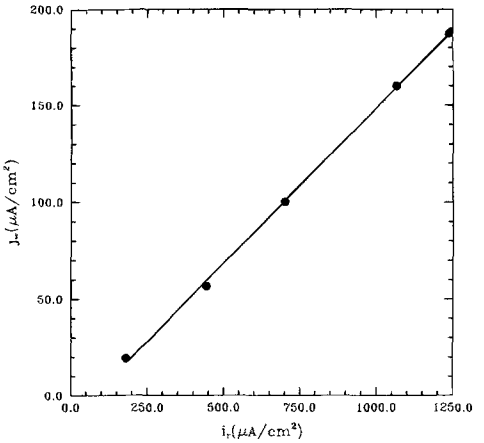

Fig. 10. Permeation current density (j_∞) *vs.* the recombination current density (i_r) in the presence of $2 \times 10^{-2}M$ of thallium ions.

The relation between the hydrogen recombination current density (i_r) and the permeation current density (j_∞) is given in Fig. 10, showing that a linear relation exists between i_r and j_∞. Obviously, the hydrogen evolution and permeation mechanism in the presence of thallium ions is different from the mechanism observed in the absence of thallium. Also the data do not fit either the modified I-P-Z model,[25] in which a linear relation should exist between ln $(i_r/\sqrt{j_\infty})$ and j_∞, or the equations derived by McBreen and Genshaw[24] for activated desorption, in which j_∞ is proportional to the square of i_c. According to Gileadi and Conway,[30] the effect of the pre-exponential terms in θ_s in Eq. 10 and 11 is negligible at intermediate values of the hydrogen surface coverage since the exponential terms in θ_s in these equations dominate the effect. Thus, Eq. 10 and 11 can be simplified

$$i_c = i_0' \, e^{-a\alpha_c\eta} e^{-\alpha_c f\theta_s} \qquad [19]$$

$$i_r = Fk_3 e^{2\alpha_c f\theta_s} \qquad [20]$$

under the Temkin isotherm assumption, Eq. 4 becomes

$$j_\infty = F(k_{abs} e^{\alpha_c f\theta_s} - k_{ads} c_s e^{-\alpha_c f\theta_s}) \qquad [21]$$

combining Eq. 3 and 21 and rearranging

$$c_s = \frac{k_{abs} e^{2\alpha_c f\theta_s}}{\frac{D}{L} e^{\alpha_c f\theta_s} + k_{ads}} = k'' e^{2\alpha_c f\theta_s} \qquad [22]$$

where $k'' = k_{abs}/D/L \; e^{\alpha_c f\theta_s} + k_{ads}$. Note that in the modified I-P-Z model,[23] Eq. 5, obtained under Langmuir assumption, was used instead of using the Temkin isotherm assumption. Substituting Eq. 22 into Eq. 3, the permeation current is obtained as

$$j_\infty = \frac{k''}{b} e^{2\alpha_c f\theta_s} \qquad [23]$$

Combining Eq. 20 and 23, one obtains

$$j_\infty = \frac{k''}{bFk_3} i_r \qquad [24]$$

Equation 24 shows that j_∞ is linearly related to i_r, which is consistent with present experimental results in the presence of thallium ions. Since $i_c = i_r + j_\infty$

$$-\frac{\partial\eta}{\partial \log i_c} = -\frac{\partial\eta}{\partial \log i_r} = -\frac{\partial\eta}{\partial \log j_\infty} \qquad [25]$$

Figure 11 shows that $\partial\eta/\partial \log i_c \approx \partial\eta/\partial \log j_\infty$, which agrees with the Eq. 25. The first two points of i_c in Fig. 11 give a slope of 126 mV/decade, which can be used to evaluate the value of i_0' under Langmuir isotherm. The calculated i_0' is 1.7 μA/cm². However, the slopes also are a function of overpotential. Again, it has been assumed that this variation is due to a mass-transfer limit. Introducing the mass-transfer term into Eq. 19 shows that

$$i_c = \left(1 - \frac{i_c}{i_l}\right) i_0' \, e^{-a\alpha\eta} e^{-\alpha f\theta_s} \qquad [26]$$

and combining Eq. 26 with Eq. 20, yields

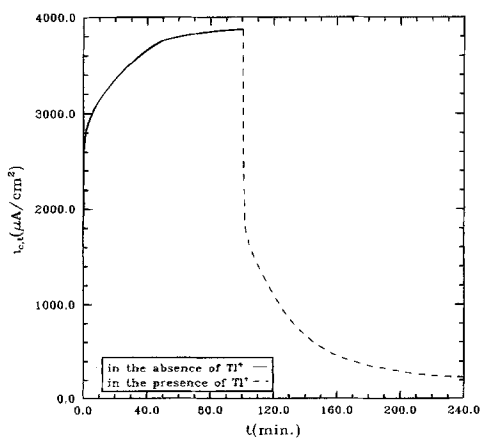

Fig. 9. Cathodic current transients on HY-130 steel membrane at applied potentials of −0.50 V *vs.* SCE in the absence and presence of $2 \times 10^{-2}M$ of Tl^+ in the electrolyte containing 0.5*M* Na_2SO_4, 0.5*M* H_2SO_4.

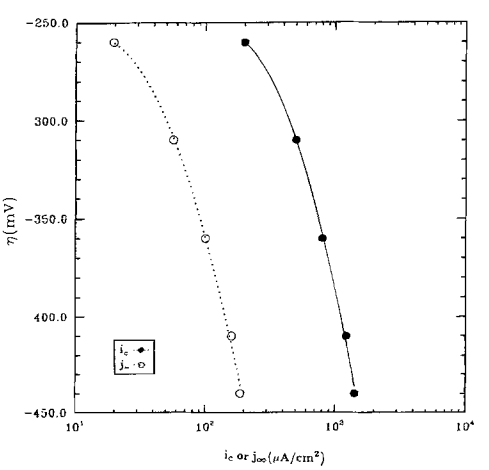

Fig. 11. The dependence of cathodic curent density (i_c) and permeation current density (j_∞) upon cathodic overpotential (η) in the presence of thallium ions.

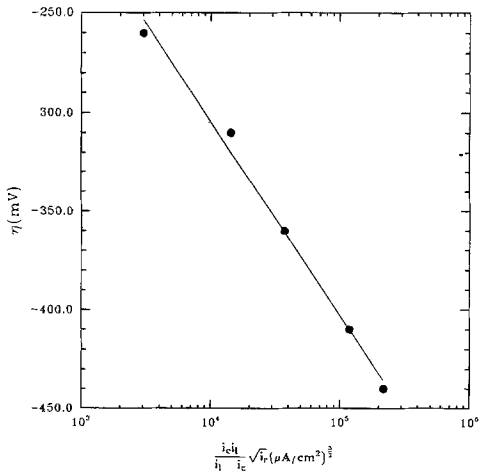

Fig. 12. $i_c i_l/(i_l - i_c)\sqrt{i_r}$ *vs.* overpotential (η) in the presence of thallium ions.

$$\log\left(\frac{i_c i_l\sqrt{i_r}}{i_l - i_c}\right) = \log\left(i_0'\sqrt{Fk_3}\right) - \frac{a\alpha\eta}{2.303} \qquad [27]$$

A limiting current density i_l of 1850 $\mu A/cm^2$ was estimated by extrapolating the experimental data given in Fig. 12. Then, using Eq. 27, the constants α_c, k_3 were calculated from the intercept and slope in Fig. 12 to be 0.59 and 2.6×10^{-10} mol/(cm^2 s), respectively. From the slope in Fig. 10, k'' was calculated to be 2.6×10^{-6} mol/cm^3. The kinetic parameters α_c, i_0', k_3, and k'' (in the presence and absence of thallium) are listed in Table I for comparison. According to Table I, the exchange current density, the recombination constant, and the absorption-adsorption constant decrease in the presence of thallium. Note that hydrogen recombination constant decreased by a factor 10^5. Consequently, the permeation current density according to Eq. 24 should increase, a phenomena observed in our experiments. The hydrogen entry efficiency, defined as j_∞/i_c%, was plotted *vs.* overpotential in Fig. 13. The hydrogen entry efficiency was increased by a factor of 10 in the presence of thallium.

The hydrogen coverages can be evaluated from Eq. 2 and 20, and the results, together with the values obtained in the absence of thallium are given in Fig. 14 as a function of overpotential. The surface coverage also increased in the presence of thallium.

Although Smialowski *et al.*[5-8] postulate that the active form of a hydrogen entry promoter is the form of hydrides, no thallium hydride formed on the steel surface under our experimental conditions as explained next. The equilibrium potential for the system Tl/TlH is $E_o = -2.107 - 0.0591$ pH $- 0.0591$ log [TlH] *vs.* SCE.[31] Thus, the experimental potentials used here were more positive than the equilibrium potential. Therefore, the atomic thallium rather than its hydride has a significant effect on the hydrogen entry, as claimed by McCright and Staehle[14] for As.

Conclusion

The absorption of thallium on steel enhances hydrogen entry. The active form of thallium acted as a hydrogen entry promoter. The observed increase in the hydrogen entry rate is due to a decrease of the hydrogen recombination rate constant. This constant was decreased by five orders of magnitude in the presence of adsorbed thallium. A mass-transfer term was introduced into the I-P-Z model to interpret the experimental results presented here. Also j_∞/i_c relationships for coupled discharge-recombination mechanism under Temkin isotherm were derived.

Table I. Kinetic parameters in the absence and presence of Tl^+.

	α_c	i_0'($\mu A/cm^2$)	k_3 (mol/cm^2 s)	k'' (mol/cm^3)
In the absence of Tl^+	0.54	18	1.1×10^{-5}	6.6×10^{-5}
In the presence of Tl^+	0.58	1.7	2.6×10^{-10}	2.6×10^{-6}

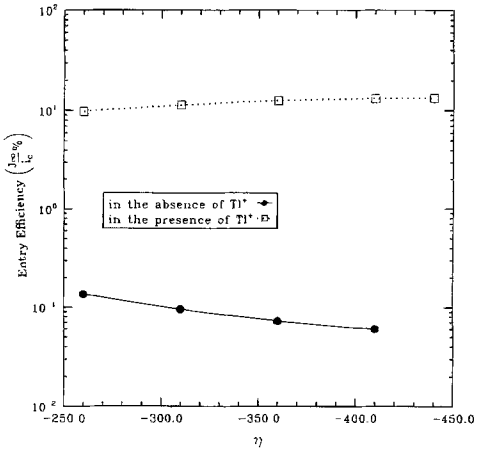

Fig. 13. Dependence of the hydrogen entry efficiency upon the overpotential (η) in the presence and absence of Tl^+.

Acknowledgment

Technical assistance and financial support by A. John Sedricks, Office of Naval Research, Contract No. N00014-92-J-1434 are gratefully acknowledged.

Manuscript submitted Oct. 22, 1993; revised manuscript received Feb. 24, 1994.

The University of South Carolina assisted in meeting the publication costs of this article.

LIST OF SYMBOLS

a	F/RT, a constant, V^{-1}
b	$L/(FD)$, a constant, equiv A cm^{-1}
c_s	surface hydrogen concentration, mol cm^{-3}
D	hydrogen diffusion coefficient, cm^2 s^{-1}
E_{app}	applied potential, V
E_c	cathodic potential, V
E^{eq}	equilibrium potential for the h.e.r., V
f	γ/RT, variable, dimensionless
F	Faraday constant, 96,487 C/equiv
L	membrane thickness, cm
i_o	the exchange current density, A/cm^2
i_0'	$i_o/1 - \theta_e$, A/cm^2
i_l	mass-transfer limiting current density, A/cm^2
i_c	cathodic current density, A/cm^2
i_r	recombination current density, A/cm^2
j_l	transition hydrogen permeation current density, A/cm^2
j_o	initial hydrogen permeation current density, A/cm^2
j_∞	steady-state hydrogen permeation current density, A/cm^2
k_{abs}	absorption rate constant, mol (cm^2 s)$^{-1}$
k_{ads}	adsorption rate constant, cm s^{-1}
k_3	recombination rate constant, mol (cm^2 s)$^{-1}$
k''	thickness dependent absorption-adsorption con-

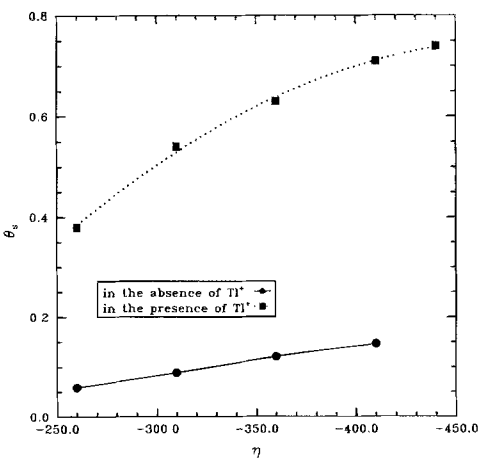

Fig. 14. Dependence of the hydrogen coverage (θ_s) upon the overpotential (η) in the presence and absence of Tl^+.

stant, $k'' = k_{abs}/k_{ads} + D/L$ for Langmuir isotherm, mol cm^{-3}

k'' $k_{abs}/k_{ads}e^{\alpha_c f\theta_s} + D/L$ thickness dependent absorption-adsorption constant for Temkin isotherm, mol cm^{-3}

R gas constant, 8.3143 J (g-mol K)$^{-1}$

T temperature, K

Greek

α_c transfer coefficient, dimensionless

θ_e hydrogen surface coverage at equilibrium, dimensionless

θ_s the hydrogen surface coverage, dimensionless

η overvoltage, $[E_{app} - E^{eq}]$, V

γ gradient of the apparent standard free energy of adsorption with hydrogen coverage, J(g-mol)$^{-1}$

REFERENCES

1. K. E. Shuler and K. J. Laidler, *J. Chem. Phys.*, **17,** 1212 (1949).
2. J. O'M. Bockris, J. McBreen, and L. Nanis, *This Journal,* **112,** 1025 (1965).
3. J. F. Newman and L. L. Shreir, *Corros. Sci.,* **9,** 631 (1969).
4. L. D. Kovba and I. A. Bagotskaya, *Zhurn. Fiz. Khim.,* **37,** 161 (1963).
5. M. Smialowski, *Hydrogen in Steel,* Addison-Wesley, Reading, MA (1962).
6. T. Zakroczymski, Z. Szklarska-Smialowski, and M. Smialowski, *Werkst. Korros.,* **26,** 61 (1975).
7. E. Lunarska, Z. Szklarska-Smialowski, and M. Smialowski, *ibid.,* **26,** 624 (1975).
8. T. Zakroczymski, Z. Szklarska-Smialowski, and M. Smialowski, *ibid.,* **27,** 625 (1976).
9. L. D. McGraw, W. E. Ditmars, C. A. Snavely, and C. L. Faust, N.A.C.A. (National Advisory Committee for Aeronautics) Technical Note 3164 (1954).
10. M. G. Fontana and R. W. Staehle, National Technical Information Service NTIS No. AD-A010 265 (1975).
11. D. O. Hayward and B. M. W. Trapnell, *Chemisorption,* p. 235, Buttersworth, London (1964).
12. H. Imai and C. Kemball, *Proc. R. Soc. London Ser. A,* **302,** 399 (1968).
13. T. P. Radhakrishnan and L. L. Shreir, *Electrochim. Acta,* **11,** 1007 (1966).
14. R. D. McCright and R. W. Staehle, *This Journal,* **121,** 609 (1973).
15. U. R. Evans, in *Scientific Principles and Practical Applications,* p. 397, Arnold, London (1961).
16. A. H. M. Aten and F. M. Zieren, *Rec. Trav. Chim.,* **49,** 641 (1930).
17. W. Beck, A. L. Glass, and E. Taylor, *This Journal,* **112,** 53 (1965).
18. V. P. Alikin, *Uchen, Zap. Perm. Gos. Univ.,* **19,** 3 (1961).
19. S. M. Beloglazov and M. I. Polukarov, *Zh. prikl. Khim.,* **33,** 389 (1960).
20. P. Subramanyan, in *Comprehensive Treatise of Electrochemistry,* Vol. 4, J. O'M. Bockris, B. E. Conway, E. Yeager, and R. E. White, Editors, p. 411, Plenum Press, New York (1981).
21. M. A. V. Devanathan and L. Strachurski, *Proc. R. Soc. London A,* **270,** 90 (1962).
22. N. Boes and H. Zuchner, *J. Less-Common Metals,* **49,** 223 (1976).
23. R. N. Iyer, H. W. Pickering, and M. Zamanzadeh, *This Journal,* **136,** 2463 (1989).
24. J. McBreen and M. A. Genshaw, in *Proceedings of the First International Symposium on Corrosion,* p. 51, held at The Ohio State University, Columbus, OH (1967).
25. R. N. Iyer, I. Takeuchi, and M. Zamanzadeh, *This Journal,* **136,** 2463 (1990).
26. J. M. Saveant and D. Tessier, *J. Electroanal. Chem.,* **65,** 57 (1975).
27. P. Sanecki, *Ind. J. Chem.,* **30A,** 225 (1991).
28. A. J. Bard and L. R. Faulkner, *Electrochemical Methods-Fundamentals and Applications,* p. 29; John Wiley & Sons, Inc., New York (1980).
29. J. O'M. Bockris and P. K. Subramanyan, *This Journal,* **118,** 1114 (1971).
30. E. Gileadi and B. E. Conway, in *Modern Aspects of Electrochemistry,* Vol. 3, J. O'M. Bockris and B. E. Conway, Editors, p. 347, Butterworths, London (1964).
31. M. Pourbaix, *Atlas of Electrochemical Equilibria in Aqueous Solutions,* Pergamon Press and Cebelcor, Brussels (1966).